Lawrence Berkeley National Laboratory

Title

Using Ice to Mimic Nacre: From Structural Materials to Artificial Bone

Permalink

https://escholarship.org/uc/item/4fc6d0hq

Authors

Deville, Sylvain
Saiz, Eduardo
Nalla, Ravi K.
et al.

Publication Date

2005-12-01

Peer reviewed

Using Ice to Mimic Nacre: From Structural Materials to Artificial Bone

Sylvain Deville, Eduardo Saiz, Ravi K. Nalla, and Antoni P. Tomsia[*]

Materials Sciences Division, Lawrence Berkeley National Laboratory,

Berkeley,CA 94720, USA

One-Sentence Summary: A natural process, freezing, is harnessed to create composites that replicate the intricate structure of a complex natural material, nacre and to synthesize porous bone substitutes with unprecedented strength up to four times higher than current state of the art materials.

Abstract: Materials that are strong, ultra light weight and tough are in demand for a range of applications, requiring architectures and components carefully designed from the meso- down to nano-scale dimensions. Nacre (seashells) and bone are frequently used as examples for how nature achieves this through hybrid organic-inorganic composites. Unfortunately, it has proven extremely difficult to transcribe nacre-like clever designs into synthetic materials partly because their intricate structures need to be replicated at several length scales. We demonstrate here how the physics of ice formation can be used to develop a whole new generation of sophisticated porous and layered-hybrid materials, including artificial bone, ceramic/metal composites and porous bone substitutes with unprecedented strength up to four times higher than those currently used for implantation, a much-needed breakthrough for fabrication of hydroxyapatite-based load-bearing orthopedic implants.

While the potential of layered materials has long been recognized, their creation requires solving a two-fold problem—the design of optimum microstructures, and

---
[*] Corresponding author: Tel: (510) 486-4918; Fax: (510) 486-4761; E-mail address: APTomsia@lbl.gov

development of fabrication procedures to implement these designs. Natural materials such as nacre offer a wealth of information to guide such a design process(*1, 2*). The unique properties of natural layered materials are achieved through a fine control of the layer thickness, selection of the right components, and manipulation of roughness and adhesion at the organic-inorganic interface(*3, 4*). The ideal fabrication process has to be not only simple but also adaptable enough to fabricate layers with a large number of material combinations and a wide range of layer dimensions. Previous techniques for mimicking nacre are bottom-up chemical approaches(*5, 6*) that are intrinsically limited to a narrow range of materials exhibiting the proper interfacial reactions and compatibility. Other techniques offer only a coarse control of the layer thickness or have practical limitations regarding the number of layers that can be fabricated(*5, 7*). Up until now, there was no method available that could replicate the interfacial chemistry, the architecture and the interfacial roughness of the shells, at the same time.

The process we introduce here is a radically new top-down approach that can be applied to a very large number of material combinations. Specifically, it is inspired by a naturally occurring phenomenon, the freezing of sea ice, which occurs at the surface of the Earth's polar oceans. In sea ice, pure hexagonal ice platelets with randomly-oriented horizontal *c* axes are formed, and the various impurities originally present in sea water (salt, biological organisms, etc.) are expelled from the forming ice and entrapped within the channels between the ice crystals(*8*). This natural segregation principle was applied here to ceramic particles dispersed in water to build sophisticated nacre-like architectures in a simple two-step approach. Porous layered material with layers as small as 1 μm are first fabricated through a novel freeze-casting process, which involves the controlled unidirectional freezing of ceramic suspensions. These porous scaffolds are then filled with a selected second phase (organic or inorganic) to fabricate dense composites. By utilizing a natural self-organizing phenomenon, we are allowing nature to guide the design and processing.

The physics of water freezing has drawn the attention of scientists for a long time. With few exceptions(*9*), the work has concentrated on the freezing of pure water of very dilute suspensions(*8, 10*). This phenomenon is critical for various applications, like cryo-preservation of biological cell suspensions(*11*) and purification of pollutants(*12*). An important conclusion of these studies is that during the freezing of such suspensions, there is a critical particle size(*10*) above which the suspended particles will be trapped by the moving water-ice front. Another important observation is that the hexagonal ice crystals exhibit strong anisotropic growth kinetics, varying over about two orders of magnitude with crystallographic orientation; under steady-state conditions, it is possible to grow ice crystals in the form of platelets, with a very high aspect ratio. The ice thus formed will have a lamellar microstructure, with the lamellae thickness depending mainly on the speed of the freezing front. We have designed a simple experimental setup that allowed us to precisely control the freezing kinetics. By freezing concentrated solutions containing ceramic particles of the right size, we were able to build homogeneous, layered, porous scaffolds.

As in nature, the ceramic particles are concentrated in the space between the ice crystals (Fig. 1a). After the ice is sublimated, the resulting scaffold is a negative replica of the ice (Fig. 1b). In addition, we have been able to control the growth of lamellar ice by adjusting the freezing kinetics. In this way, we have achieved a layered microstructure with relevant dimensions that vary over two decades, from 1 μm (almost the same as nacre, typically ~0.5 μm)(*13*) to 200 μm (Fig. 2), without affecting the ordered architecture.

The scaffold materials obtained by this process exhibit striking similarities with the meso- and micro- structure of the inorganic component of nacre (Fig. 1). The inorganic layers are parallel to each other and very homogeneous throughout the entire sample. Particles trapped in between the ice dendrites (Fig. 1a) led to a dendritic surface

roughness of the walls (Fig. 1b), just as in nacre(*14*). Finally, some dendrites span the channels between the lamellae (Fig. 2a), mimicking the tiny inorganic bridges linking the inorganic platelets of nacre, which are believed to increase the fracture resistance(*15*).

The inorganic portion represents 95 vol.% of nacre, but its highly specific properties are due to the remaining 5%, the organic phase (protein) that is found between the calcium carbonate platelets(*13*). Hence, to obtain similar synthetic materials, the next step is to fill the porous ceramic scaffolds with a second phase. For example, we have filled the scaffolds with a simple organic phase (epoxy, Fig. 1c) or with an inorganic component (metal, Fig. 1d). Nature shows that the optimum fracture properties are encountered not only when the organic/inorganic interface is strong, but also when delamination at the organic/inorganic interface occurs before the crack goes across the stiff, brittle layer. It is believed that nature manipulates adhesion in two ways− mechanical and chemical. In nacre, this is done by controlling the roughness and the highly specific properties of the polymer adhesive phase(*3*). Our process allows us to control the morphology of the inorganic layers and the chemistry of the interface. For example, the mechanical response of alumina/aluminum layered composites (Fig. 1d) can be manipulated by controlling the interfacial bonding; specifically, by adding as little as 0.5 wt.% Ti to the aluminum eutectic (known to segregate at the metal/ceramic interfaces(*16*)), the strength increases from 400 to 600 MPa and fracture toughness from 5.5 to 10 MPa√m (Fig. 1e).

Our technique shows promise for a large number of applications that require tailored composite materials. One such scientific challenge that could be solved is the development of new biomaterials for orthopedic applications(*17*). Despite extensive efforts in the development of porous scaffolds for bone regeneration, all porous materials have a common, fundamental limitation− the inherent lack of strength

associated with porosity. So, the unresolved dilemma is how we design and create a scaffold that is both porous and strong. By applying freeze casting to commercial hydroxyapatite (HAP) powder, the mineral component of bone, we processed highly porous lamellar scaffolds that are four times stronger than conventional porous HAP (Fig. 3). These scaffolds exhibit well-defined pore connectivity along with directional and completely open porosity. Hence, most of the current shortcomings (low strength, random organization, multiple pore size, uncontrolled pore connectivity) that plague such bone substitutes are solved by this innovative approach.

Current ceramic and metallic implant materials have serious shortcomings due to the mismatch of physical properties with those of bone, where intrinsically weak materials such as calcium phosphates and collagen are combined in to composites exhibiting intermediate modulus (10-20 GPa), fairly high strength (30 to 200 MPa) and high work of fracture (100-1000 J/m^2)(*18*). The unique properties of bone arise from the controlled integration of the organic (collagen) and inorganic (apatite) components(*4*), with a sophisticated architecture from the nano- to the meso- levels. Many researchers have tried to create bone-like materials, but that has proven to be a daunting task. Our approach is to combine biomimetics with a new design philosophy, producing dense and strong bioactive bodies—intended to be partially or completely resorbed and replaced by the surrounding bone tissue over time. This can be accomplished by infiltrating the lamellar porous HAP scaffolds fabricated here with a second organic phase with tailored biodegradability. Because the biodegradation rates of the scaffold and the infiltrated compound can be designed to be different, porosity will be created *in situ* to allow bone ingrowth.

Our results show that this approach can be applied to follow the nacre microstructure paradigm, designing HAP-based composites with stiffness (10 GPa), strength (150 MPa) and work of fracture (220 J/m^2) matching that of bone, for an

equivalent mineral/organic content. In addition, the mesostructure of bone determines, to a great extent, its mechanical response—something that cannot be replicated with current chemical bottom-up approaches. However, our results indicate that by controlling the freezing kinetics and the patterns of the cold finger, it is also possible to build mesostructural features and gradients (Fig. 4d) much like cortical bone (Fig. 4e). Clearly, this is the first step in producing a whole new generation of biomaterials that truly mimic bone at all levels.

In this work, a natural process, freezing, is harnessed to create composites which replicate the intricate structure of a complex natural material, nacre. Natural materials are limited to a few components—calcium carbonates, phosphates, iron and silica. Our process, on the other hand, is a very versatile and efficient method that can utilize a much broader range of components for producing a new generation of biomimetic composites, from artificial bone to metal/ceramic seashells. This research has revealed aspects of the freezing of concentrated solutions that are relevant in fields as diverse as physics, biology and earth sciences, while the microstructures and unique properties of the composites will be of interest to those working in the multidisciplinary fields of materials science and biomimetics.
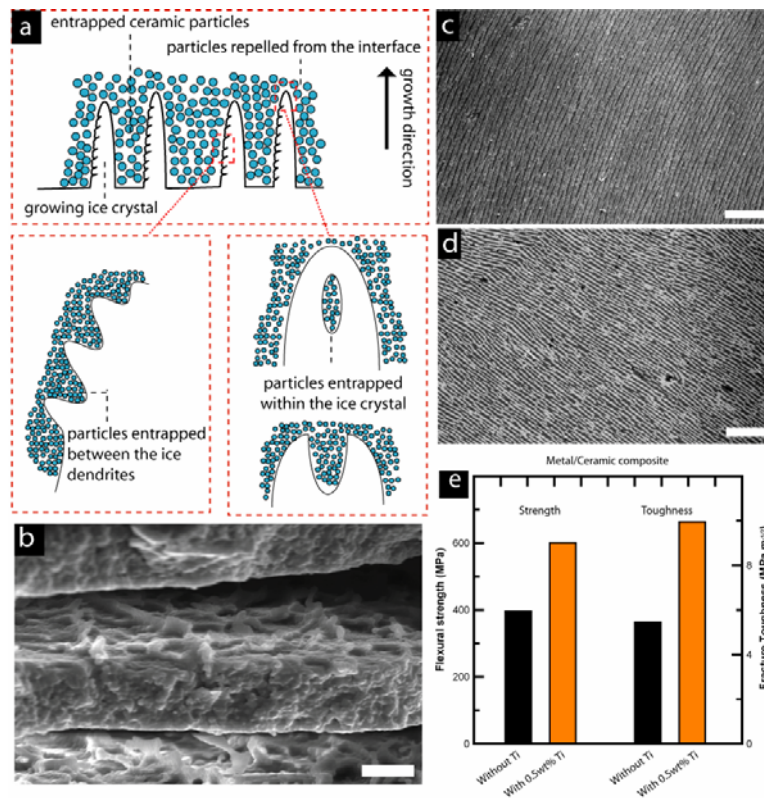
Acknowledgments

Figure 1. **Processing principles, materials and properties**. While the ceramic slurry is freezing, the growing ice crystals expel the ceramic particles creating a lamellar microstructure oriented in a direction parallel to the movement of the freezing front. (a). Particles entrapped between the ice dendrites generate a characteristic roughness on the lamella surface (b). Unlike for dilute suspensions, for highly concentrated slurries the interaction between particles becomes critical: a small fraction of particles are entrapped within the ice crystals by tip-splitting and subsequent healing (a), forming ceramic bridges between layers (e.g. Fig. 2a). Dense composites are obtained by infiltrating the porous lamellar ceramic with a second phase (e.g. a polymer or a liquid metal). Typical composite microstructures are shown in the scanning electron micrographs: (c) alumina/epoxy and (d) alumina/(Al-Si eutectic). The two distinctive features generated during freezing (interfacial roughness and ceramic bridges) mirror the "brick, mortar and bridges" nacre microstructure and provide unique properties. A large contribution to toughness in nacre comes from controlling adhesion at the

organic/inorganic interface. A similar degree of control can be achieved here: (e) strength and toughness of aluminium/alumina composites are drastically improved by engineering the metal/ceramic interface adding 0.5wt% Ti to aluminium. Scale bars (b) 10 μm (c) 500 μm (d) 300 μm.
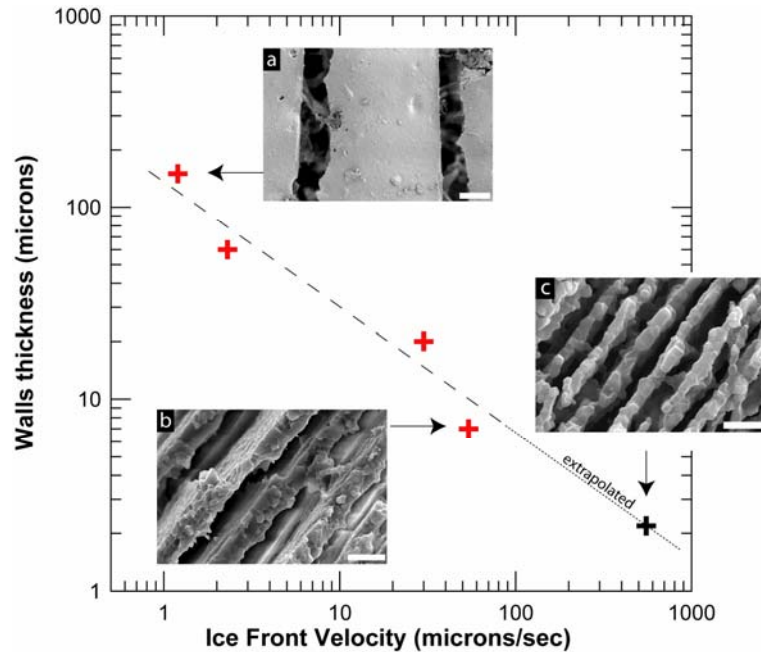
Figure 2. **Control at the microstructural size scale**. Data and scanning electron micrographs showing the effect of varying the cooling rate on the microstructure. Cross-sections were taken parallel to the ice front for alumina samples with solidification-front speeds of (a) 1.2 μm/s and (b) 54 μm/s. Sample (c) was obtained with ultrafast freezing to gauge the thickness limit achievable by this technique. The approximate ice front velocity for this extreme case is in agreement with the extrapolation of the controlled freezing results. The solidification-front speed was modified by changing the temperature gradient and the cooling kinetics. When the freezing rate increases, the magnitude of supercooling ahead of the solidifying interface is increased, and as a result the tip radius of the ice crystals decreases. A finer microstructure is thus obtained, without affecting the long range order of the entire structure. Scale bars (a) 50 μm (b) 10 μm (c) 5 μm.
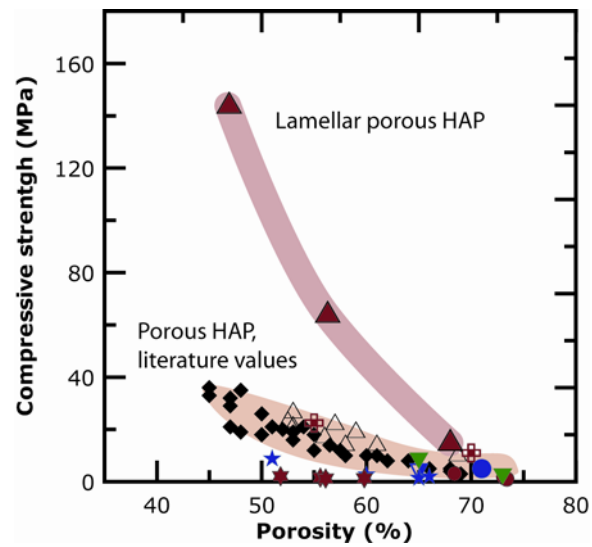
Figure 3. **Compressive strength of porous hydroxyapatite scaffolds**. Results from literature (*19-27*) vs. lamellar porous hydroxyapatite scaffolds produced here that show promise as bone substitute materials. For the lamellar material, compression is applied in the direction parallel to the ceramic layers. Each style of points corresponds to a different source of the literature.
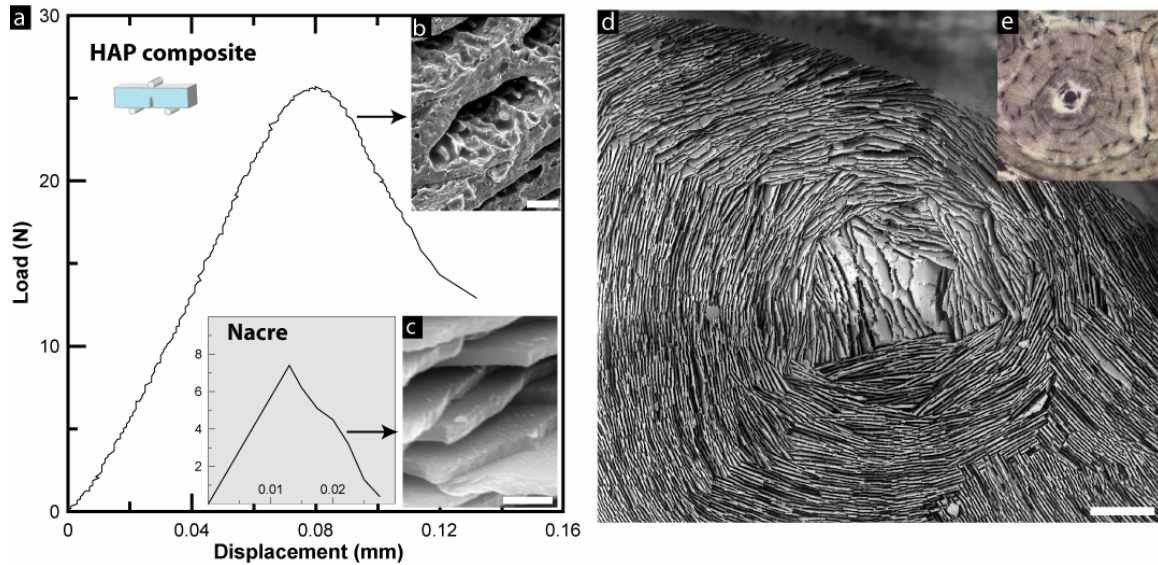
Figure 4. **Comparison of natural and synthetic materials**. The load-displacement data for the HA composites (a) was qualitatively very similar to that of nacre (c) (*15*), showing evidence of stable crack propagation, unlike ceramics which fracture in a brittle manner (load-displacement data is linear up to failure). In both cases, ceramics platelets are lying perpendicularly to the loading direction. Typical scanning electron micrographs of the synthetic materials (b) and abalone shell (c) reveal similar features on the fracture surface, with crack deflection along the interface, providing a significant toughening contribution. In addition, control of the mesostructure is also possible, e.g. in alumina (d) by patterning the surface of the cold fingers on which the ice crystals grow. Mesostructure similar to osteonal bone can be obtained (human cortical bone in inset(*28*)). Scale bars (b) 40 μm (c) 1 μm (d) 500 μm.

References

1. C. Sanchez, H. Arribart, M. M. G. Guille, *Nature Materials* **4**, 277-288 (2005).
2. L. Addadi, S. Weiner, *Nature* **389**, 912 (1997).
3. B. L. Smith *et al.*, *Nature* **399**, 761-763 (1999).
4. G. E. Fantner, Hassenkam, T., Kindt, J. H., Weaver, J. C., Birkedal, H., Pechenik, L., Cutroni, J. A., Cidade, G. A. G., Stucky, G. D., Morse, D. E., Hansma, P. K., *Nature Materials* **4**, 612-616 (2005).
5. Z. Y. Tang, N. A. Kotov, S. Magonov, B. Ozturk, *Nature Materials* **2**, 413-418 (2003).
6. A. Sellinger *et al.*, *Nature* **394**, 256-260 (1998).
7. W. J. Clegg, *Science* **286**, 1097 (1999).
8. M. G. Worster, J. S. Wettlaufer, *Journal of Physical Chemistry B* **101**, 6132-6136 (1997).
9. T. Fukasawa, Z. Y. Deng, M. Ando, T. Ohji, Y. Goto, *Journal of Materials Science* **36**, 2523-2527 (2001).
10. H. Ishiguro, Rubinsky, B., *Cryobiology* **31**, 483-500 (1994).
11. J. O. M. Karlsson, *Science* **296**, 655-656 (2002).
12. G. Gay, M. A. Azouni, *Crystal Growth & Design* **2**, 135-140 (2002).
13. A. P. Jackson, Vincent, J.F.V, Turner, R.M., *Proc R Soc London B* **234**, 415-440 (1988).
14. R. Z. Wang, Z. Suo, A. G. Evans, N. Yao, I. A. Aksay, *Journal of Materials Research* **16**, 2485-2493 (2001).
15. F. Song, A. K. Soh, Y. L. Bai, *Biomaterials* **24**, 3623-3631 (2003).
16. E. Saiz, R. M. Cannon, A. P. Tomsia, *Acta Materialia* **48**, 4449-4462 (2000).
17. L. L. Hench, J. M. Polak, *Science* **295**, 1014 (2002).
18. Y. H. An, in *Mechanical testing of bone and the bone-implant interface*. (CRC Press, Boca Raton, 2000) pp. 41-63.
19. A. Almirall *et al.*, *Biomaterials* **25**, 3671-3680 (2004).
20. R. P. del Real, J. G. C. Wolke, M. Vallet-Regi, J. A. Jansen, *Biomaterials* **23**, 3673-3680 (2002).
21. J. C. Lehuec, T. Schaeverbeke, D. Clement, J. Faber, A. Lerebeller, *Biomaterials* **16**, 113-118 (1995).
22. H. R. Ramay, M. Q. Zhang, *Biomaterials* **24**, 3293-3302 (2003).
23. A. Bignon, *Optimization of the porous structure of calcium phosphate implants for bone substitutes and in situ release of active principles*, Phd Report, Materials Science Department (National Institute of Applied Science, Lyon, 2002).
24. M. Sous *et al.*, *Biomaterials* **19**, 2147-2153 (1998).
25. D. M. Liu, *Ceramics International* **23**, 135-139 (1997).
26. M. Milosevski, J. Bossert, D. Milosevski, N. Gruevska, *Ceramics International* **25**, 693-696 (1999).
27. M. Kawata *et al.*, *Journal of Materials Science-Materials in Medicine* **15**, 817-823 (2004).
28. J. Crimando, *http://www.gwc.maricopa.edu/class/bio201/histoprc/prac3q.htm* (1997, accessed 08/26/2005), vol. 2005.

Supporting Online Materials (Materials and Methods)
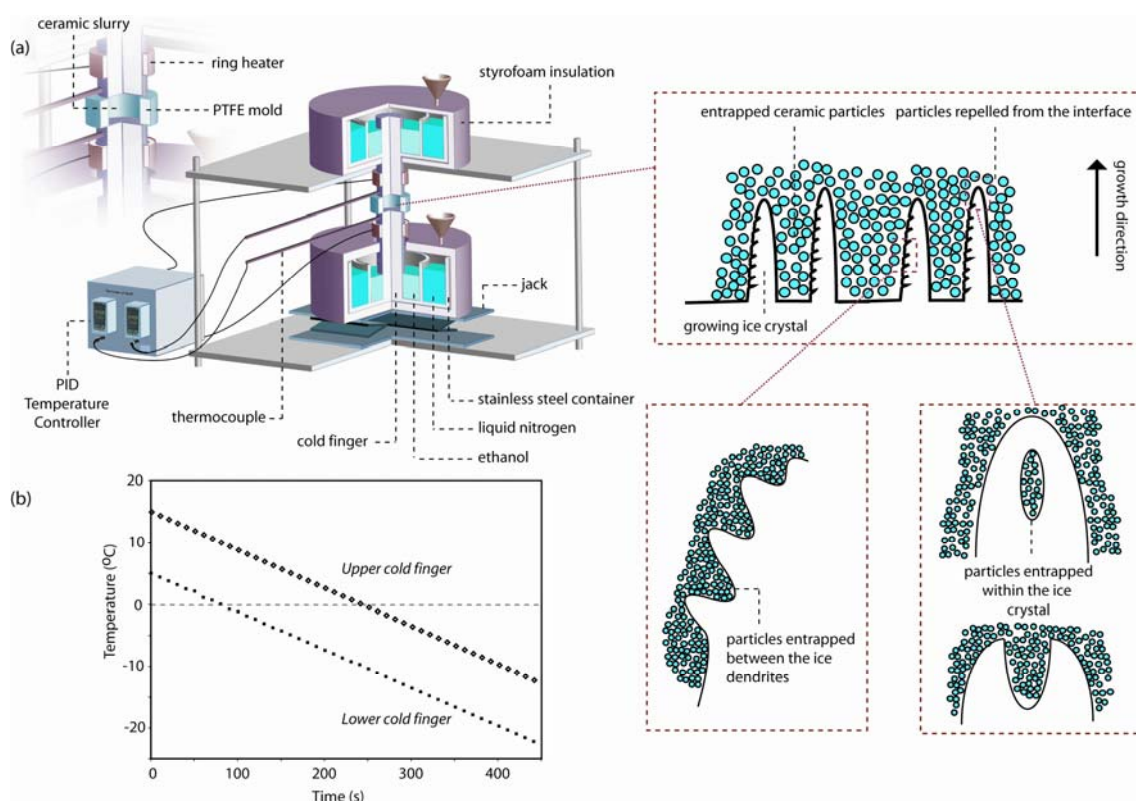
Porous inorganic scaffolds were produced by controlled unidirectional freezing of ceramic slurries. Slurries were prepared by mixing distilled water with a small amount (typically 1 wt.%) of ammonium polymethacrylate anionic dispersant (Darvan C or Darvan 811, R. T. Vanderbilt Co., Norwalk, CT), an organic binder (PVA) and the inorganic material powder in various content (Alumina powder: Ceralox SPA05, Ceralox Div., Condea Vista Co., Tucson, AZ; HAP powder: Hydroxyapatite#30, Trans-Tech, Adamstown, MD). Slurries were ball-milled for 20 hrs with alumina balls and de-aired by stirring in a vacuum dessicator. Freezing of the slurries was done by pouring them into a teflon mold, with two copper rods on each side which were cooled using liquid nitrogen (Fig. 1). Freezing kinetics were controlled by heaters placed on the metallic rods and thermocouples placed on each side of the mold. Frozen samples were freeze dried (Freeze dryer 8, Labconco, Kansas City, MI) at low temperature (-100°C) and pressure (1300 Pa), for 24 hrs. Sintering of the green bodies thus produced was

done in an air furnace (1216BL, CM Furnaces Inc., Bloomfield, NJ), with dwell temperatures depending on the ceramics used (2 h at 1500°C for alumina, 3 h at 1350°C for HAP). The scaffolds were then infiltrated to obtain composite materials. For example, epoxy infiltration was done by embedding the porous ceramics scaffolds in a standard epoxy resin (Epoes, Struers, Westlake, OH) under vacuum. Aluminum infiltration was done by dipping the porous alumina scaffold into aluminum alloy, melted *in vaccuo,* under a gas pressure of 40 kPa.

The (bending) strength tests involved loading unnotched, nominally flaw-free, beams ~2 x 2 x 15 mm sectioned from the composites, to failure at a rate of ~0.015 mm/sec under three-point bending (center-to-end loading span = 10.15 mm) using a standard mechanical testing machine; the load-displacement data thus obtained were analyzed to assess the (ultimate) bending strength. Fracture toughness testing was performed in general accordance with ASTM Standard E-399 for Plane-Strain Fracture Toughness (1). Beams ~2 x 3 x 15 mm were sectioned, then notched to a depth of ~1.5 mm using a slow-speed saw before being sharpened with a razor blade. The samples were loaded to failure at a rate of ~0.015 mm/sec under three-point bending using the mechanical testing machine. The load-displacement data obtained were analyzed to assess the fracture resistance which was assessed in terms of the fracture toughness and the work-of-fracture (from area under the load-displacement curve).

1. ASTM-E399-90, in *Annual Book of ASTM Standards*. (West Conshohocken, Pennsylvania, USA, 2002), vol. 03.01: Metals- Mechanical Testing; Elevated and Low-temperature Tests; Metallography ASTM.